A challenge problem for detection of targets in foliage

Mikael Lundberg[*a], Lars M. H. Ulander[a], William E. Pierson[b], Anders Gustavsson[a]
[a]Department of Radar Systems, Swedish Defence Research Agency (FOI),
P.O. Box 1165, SE-581 11 Linköping, Sweden;
[b]Air Force Research Lab / SNAA, 2241 Avionics Circle, Wright-Patterson AFB, OH 45433

ABSTRACT

This paper describes a challenge problem whose scope is detection of stationary vehicles in foliage using VHF-band SAR data. The data for this challenge problem consists of images collected by the Swedish CARABAS-II system which produces SAR images at the low VHF-band (20-90 MHz). At these frequencies the electromagnetic energy from the radar penetrates the foliage of the forest, providing a return from a target concealed in a forest. Thus, VHF-band SAR technology transforms the foliage penetration problem into a traditional detection problem where the goal is to reduce the false alarm rate (FAR). Reducing the FAR requires suppressing the clutter in a VHF-band SAR image which is dominated by larger tree trunks, buildings and other man-made objects. The purpose of releasing the CARABAS-II data set is to provide the community with VHF-band SAR data that supports development of new algorithms for robust target detection with a low false alarm rate. The set of images supports single-pass, two-pass and multi-pass target detection.

Keywords: Challenge Problem, VHF SAR, CARABAS-II, Change Detection

1. INTRODUCTION

This paper presents a challenge problem and a data set for detection of targets concealed by forest. The main objective is to provide the community with a publicly available VHF-band SAR data set which can be used to develop new detection methods and generate results for publication. The data consists of SAR images collected with the Swedish low VHF-band SAR system CARABAS-II. These images are a subset of images that were collected during a flight campaign held 2002 in northern Sweden whose purpose was to acquire data supporting change detection for different operating conditions. The paper addresses the three components of a challenge problem; problem definition, data description and baseline performance.

2. PROBLEM DEFINITION

In many situations where there is a need to find and monitor vehicles over a large area the problem of detecting targets concealed by foliage appears. A low frequency SAR system combines the capabilities of wide area surveillance and good foliage penetration making it a sensor well suited to solve the problem. At the low VHF-band most energy is transmitted through the forest canopy and the main radar backscatter comes from large scatterers such as tree trunks, boulders, houses and other man-made objects. Larger vehicles will also show high levels of backscatter making them appear as bright objects in a SAR image.

The main technical challenge associated with designing an automated detection algorithm is not detecting targets but sufficiently suppress the clutter to give a false alarm rate low enough to be useful to the operator. The dominating source of clutter for detection of targets in foliage using VHF-band SAR images is the backscatter from larger tree trunks. In sparse forests with thin trees it might be possible to detect vehicles in a single image with few false alarms because the signals from targets are larger than from the clutter. However, in old and dense forests with large trees it can be difficult discriminating a target from the background clutter.

Since the objects that dominate the clutter are large and normally stationary their radar signatures are very stable between different image acquisitions. Hence, a combination of SAR images from different flight passes can be used to suppress

[*] mikael.lundberg@foi.se; phone +46 13 378556; fax +46 13 378488

Algorithms for Synthetic Aperture Radar Imagery XIII, edited by Edmund G. Zelnio, Frederick D. Garber,
Proc. of SPIE Vol. 6237, 62370K, (2006) · 0277-786X/06/$15 · doi: 10.1117/12.663594

clutter significantly. Change detection on VHF-band SAR images has shown good performance of detecting targets under trees [1][2]. However, few SAR systems working in the low VHF-band exist. Consequently, few researchers have had access to such data. By releasing a VHF-band SAR image data set to the public more researchers can be part of developing new change detection algorithms.

3. DATA DESCRIPTION

3.1 CARABAS-II VHF SAR

CARABAS-II is the second-generation airborne ultra-wideband SAR designed and operated by the Swedish Defence Research Agency (FOI) [3]. The system transmits HH-polarized radio waves between 20-90 MHz, corresponding to wavelengths between 3.3 m and 15 m. When using the full signal bandwidth and an azimuth integration angle of about 70° a resolution in the order of 2.5 m by 2.5 m is obtained in the slant range image plane.

The platform that hosts the sensor is a Sabreliner aircraft, as seen in Figure 1. The raw radar data are recorded to hard drives onboard while all signal processing such as image formation, radiometric calibration, geo-coding, and change detection are performed off-line in the laboratory.

The CARABAS-II waveform is a stepped-frequency signal which consists of chirp pulses with nominally 2 MHz bandwidth. The (sub-band) pulse echoes are used to synthesise an equivalent wide-band pulse echo [4]. The system parameters commonly used by CARABAS-II during flight missions are shown in Table 1.

Figure 1. The CARABAS-II VHF SAR in operation with the antennas deployed in the front of a Sabreliner aircraft (© Photo: Pia Ericson, FMV).

Table 1. Common radar parameters used by CARABAS-II.

System Parameter	Value	System Parameter	Value
Nominal flight altitude	3 - 9 km	Frequency step	1.875 MHz
Nominal flight speed	127 m/s	Centre frequencies	21.25 - 85 MHz
Frequency band	20 - 86 MHz	Pulse repetition frequency	5000 Hz
Aperture angle	90°	Pulse length	5 - 15 μs
Transmitted power (peak)	500 W	Maximum range	26.4 km
Pulse modulation	Non-linear FM		
Frequency sub-bands	35 (+ 1 RFI sniff)		

3.2 Data collection

The data provided for this challenge problem was collected during a large-scale flight campaign held in Sweden during the early summer of 2002. The objective for the campaign was to collect VHF SAR data to provide a large image set to evaluate the performance of VHF-band change detection of targets obscured by foliage. For this purpose seventeen missions were conducted resulting in 150 flight passes over the ground test area. Data was collected to cover a range of operating conditions affecting change detection performance, such as incidence angle, heading difference between the two images used to form a change image, target orientation, target size and RFI (radio frequency interference) [5][6].

The site used for the SAR measurements was the military test range RFN Vidsel located in the far north of Sweden. This test site included mostly forested areas but also lakes, fields and buildings. The image to the left in Figure 2 shows a map of Sweden pointing out the location of RFN Vidsel. The image to the right is an aerial photo showing a smaller region of the test site which was used as the main area for target deployments.

During the campaign seven target deployments were arranged. One was established on an open field while the remaining six were established in the forest. Two smaller sites in the area were chosen for the six target deployments under foliage. The locations of these forest areas are marked with white rings in the right image in Figure 2. Forest 1 is located just west of the northern limit of the lake and forest 2 is situated approximately 2.5 km north of forest 1. The dominating tree species in the area was Scots pine. Due to the northern location, the forests were sparse with stand volumes of 113 m^3/ha and 81 m^3/ha in forest 1 and 2, respectively. In each forest site 50 positions were selected as potential points to locate a target. These positions were measured using a GPS receiver to facilitate the following detection analysis [7][8].

The targets consisted of 25 terrain vehicles in three sizes; ten TGB11 with dimensions 4.4x1.9x2.2 m, eight TGB30 with dimensions 6.8x2.5x3.0 m and seven TGB40 with dimensions 7.8x2.5x3.0 m (length x width x height). Figure 3 shows the three vehicle types deployed in forest 1. The smallest vehicle is the TGB11 which has a box-like design. TGB30 and TGB40 are truck-sized vehicles. The main difference between the two is that TGB40 has an additional rear wheel axis making it one meter longer than the TGB30.

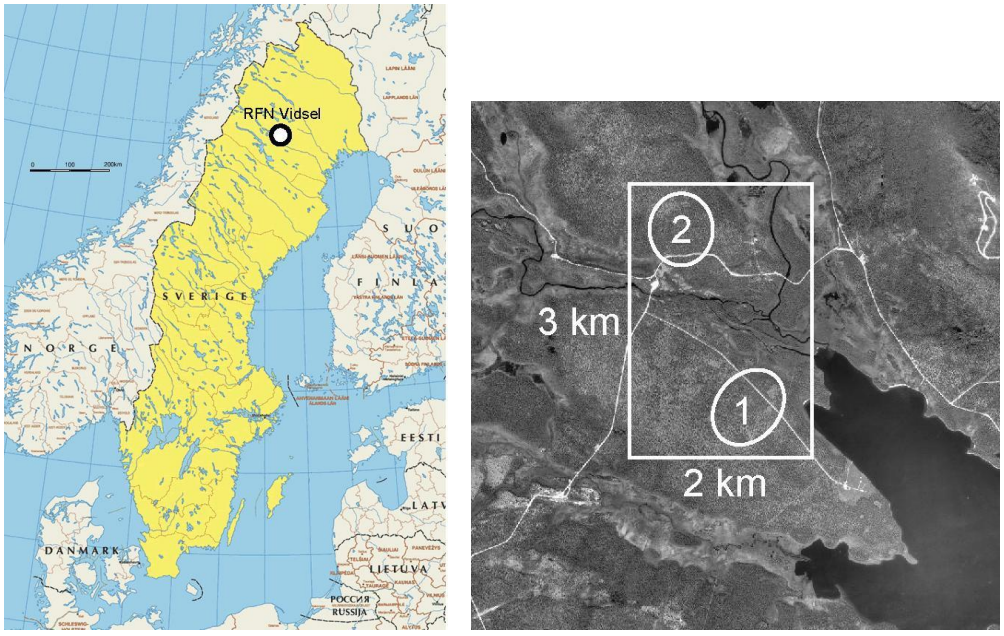

Figure 2. Left: Map of Scandinavia. The white circle in northern Sweden shows the location of the military test range RFN Vidsel. (© Map: Europeiska kommissionen). Right: Aerial photo of the main test area inside RFN Vidsel. The white rings show the two forest sites used for concealed target deployments. (© Aerial photo: Lantmäteriverket Gävle 2006. Ref. no. I 2006/719).

Figure 3. Terrain vehicles used as targets during the experiment. Left: TGB11. Middle: TGB30. Right: TGB40. These images also reflect the typical characteristics of forest site 1.

3.3 Data set

Of all the CARABAS-II data that were collected during the flight campaign in Vidsel 2002, a sub set of 24 images has been selected for public release. These images were acquired in four separate flight missions, called v02_2, v02_3, v02_4 and v02_5, where v02 stands for Vidsel 2002 and the added index corresponds to the mission number. From each of the four missions, six images were chosen to form the 24 images available in this data set.

Three imaging geometries were used repeatedly during the collection of the images. In each set of six images two images were acquired with a flight heading of 225°, two with heading 135° and two with heading 230°. The heading is defined as 0° pointing towards north with clock-wise increasing heading. CARABAS-II used a left looking mode meaning that the radar was transmitting in the directions 135°, 45° and 140°. All images were measured in strip map SAR mode having a range of 12 km to a common aim point. The incidence angle to the aim point was 58°. The closest source of RFI was a TV transmitter located south-east of the test area. This makes the images collected with flight headings 225° and 230° more affected by RFI, since the main lobe is then pointing towards the TV transmitter.

Four target deployments; Sigismund, Karl, Fredrik and Adolf-Fredrik (named after Swedish kings) are associated with the four flight missions. In deployment Sigismund the targets were placed close to the road in forest 2 in a 5 by 5 target array. The spacing between the vehicles was approximately 50 m. All vehicles were oriented with the front pointing south-west. Deployment Karl was also located in forest 2, but with the target array moved to the north of deployment Sigismund. Here the fronts of the vehicles were rotated to point towards north-west. The two remaining deployments were established in forest site 1. In deployment Fredrik the targets were placed close to the road and oriented in a south-western heading. The vehicles were then moved away from the road and deployed with the fronts pointing to the west for deployment Adolf-Fredrik. Figure 4 to Figure 7 show sketches of each of the four target deployments.

The data set consists of 24 magnitude SAR images where the phase information has been removed by taking the absolute value of the data. Each image has been geo-referenced to the Swedish reference system RR92 [9][10] and covers an area of size 2 km x 3 km, corresponding to the white rectangle in the right image in Figure 2. The pixel size is 1 m x 1 m making the image data having 3000 rows and 2000 columns. Table 2 summarizes the operating conditions associated with each image in the data set.

Table 2. Operating conditions associated with each image in the data set.

Image file name	Flight Heading (deg)	Incidence Angle (deg)	RFI	Deployment	Forest Site	Target heading (deg)
			0=Low 1=High			
v02_2_1_1.a.Fbp.RFcorr.Geo.Magn	225	58	1	Sigismund	2	225
v02_2_2_1.a.Fbp.RFcorr.Geo.Magn	135	58	0	Sigismund	2	225
v02_2_3_1.a.Fbp.RFcorr.Geo.Magn	225	58	1	Sigismund	2	225
v02_2_4_1.a.Fbp.RFcorr.Geo.Magn	135	58	0	Sigismund	2	225
v02_2_5_1.a.Fbp.RFcorr.Geo.Magn	230	58	1	Sigismund	2	225
v02_2_6_1.a.Fbp.RFcorr.Geo.Magn	230	58	1	Sigismund	2	225
v02_3_1_2.a.Fbp.RFcorr.Geo.Magn	225	58	1	Karl	2	315
v02_3_2_1.a.Fbp.RFcorr.Geo.Magn	135	58	0	Karl	2	315
v02_3_3_1.a.Fbp.RFcorr.Geo.Magn	225	58	1	Karl	2	315
v02_3_4_1.a.Fbp.RFcorr.Geo.Magn	135	58	0	Karl	2	315
v02_3_5_2.a.Fbp.RFcorr.Geo.Magn	230	58	1	Karl	2	315
v02_3_6_1.a.Fbp.RFcorr.Geo.Magn	230	58	1	Karl	2	315
v02_4_1_1.a.Fbp.RFcorr.Geo.Magn	225	58	1	Fredrik	1	225
v02_4_2_1.a.Fbp.RFcorr.Geo.Magn	135	58	0	Fredrik	1	225
v02_4_3_1.a.Fbp.RFcorr.Geo.Magn	225	58	1	Fredrik	1	225
v02_4_4_1.a.Fbp.RFcorr.Geo.Magn	135	58	0	Fredrik	1	225
v02_4_5_1.a.Fbp.RFcorr.Geo.Magn	230	58	1	Fredrik	1	225
v02_4_6_1.a.Fbp.RFcorr.Geo.Magn	230	58	1	Fredrik	1	225
v02_5_1_1.a.Fbp.RFcorr.Geo.Magn	225	58	1	Adolf-Fredrik	1	270
v02_5_2_1.a.Fbp.RFcorr.Geo.Magn	135	58	0	Adolf-Fredrik	1	270
v02_5_3_1.a.Fbp.RFcorr.Geo.Magn	225	58	1	Adolf-Fredrik	1	270
v02_5_4_1.a.Fbp.RFcorr.Geo.Magn	135	58	0	Adolf-Fredrik	1	270
v02_5_5_1.a.Fbp.RFcorr.Geo.Magn	230	58	1	Adolf-Fredrik	1	270
v02_5_6_1.a.Fbp.RFcorr.Geo.Magn	230	58	1	Adolf-Fredrik	1	270

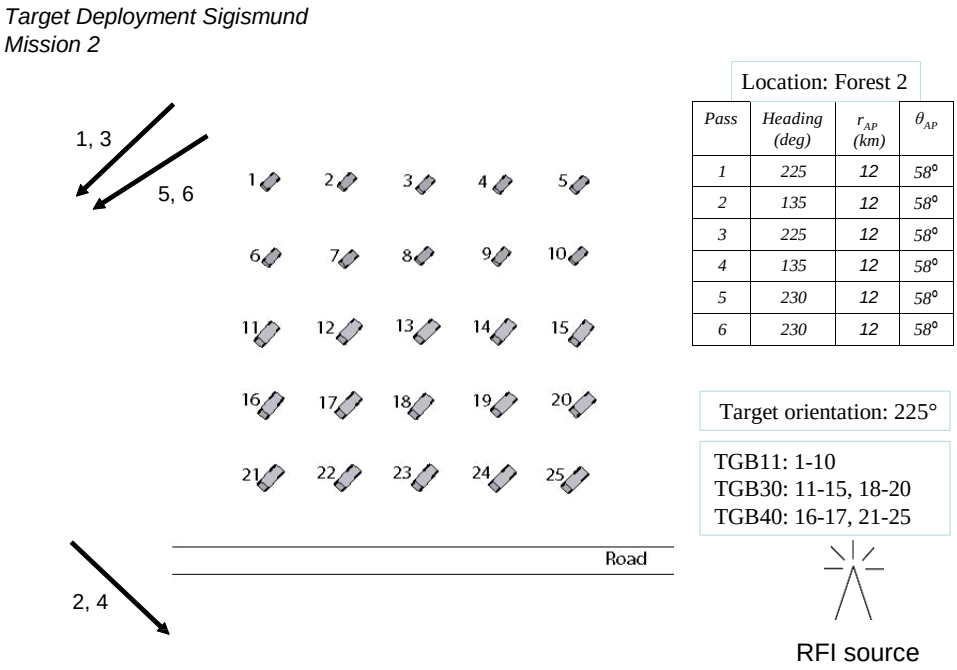

Figure 4. Sketch of deployment Sigismund showing the approximate location of the targets. The vehicles were oriented in a south-western heading. Arrows show the directions of the flight passes during mission 2. To the right is a table explaining the geometry for each flight pass. Individual targets are marked with a number (1 to 25) and a list associates the target number with target type.

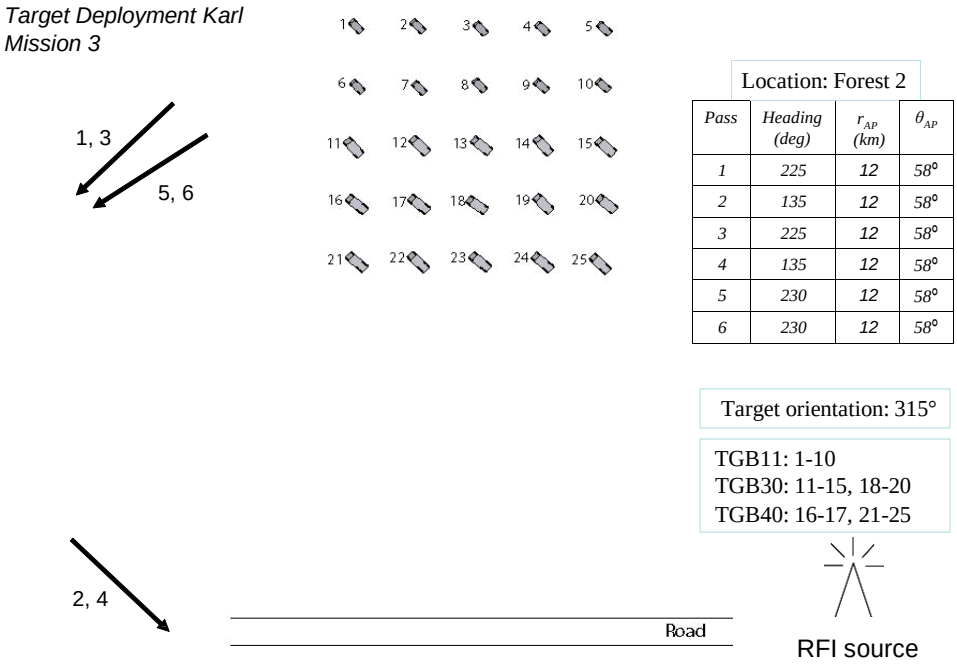

Figure 5. Sketch of deployment Karl showing the approximate location of the targets. The vehicles were oriented in a north-western heading. Arrows show the directions of the flight passes during mission 3. To the right is a table explaining the geometry for each flight pass. Individual targets are marked with a number (1 to 25) and a list associates the target number with target type.

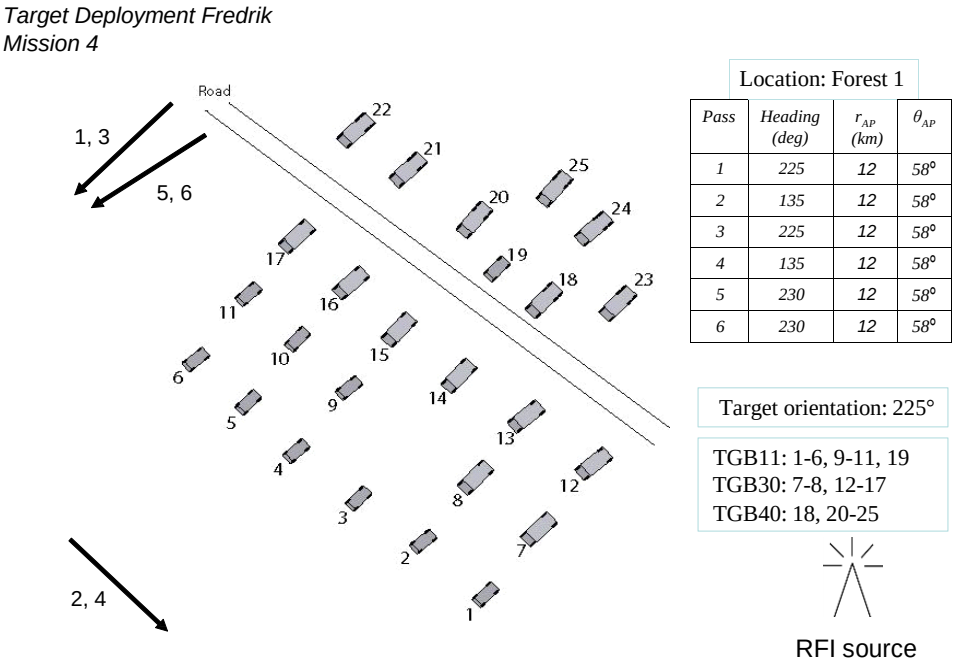

Figure 6. Sketch of deployment Fredrik showing the approximate location of the targets. The vehicles were oriented in a south-western heading. Arrows show the directions of the flight passes during mission 4. To the right is a table explaining the geometry for each flight pass. Individual targets are marked with a number (1 to 25) and a list associates the target number with target type.

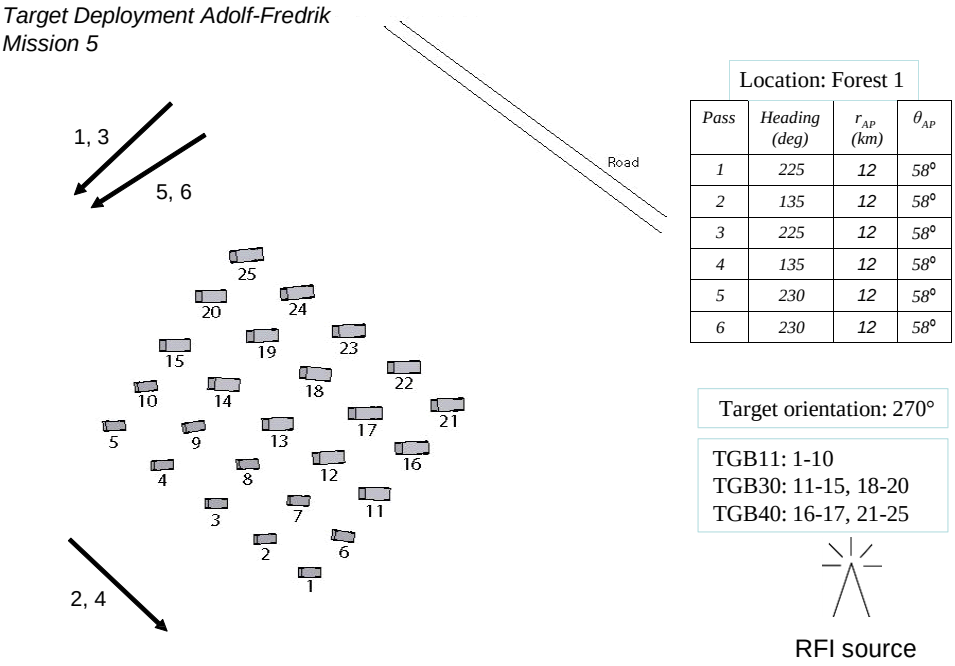

Figure 7. Sketch of deployment Adolf-Fredrik showing the approximate location of the targets. The vehicles were oriented in a western heading. Arrows show the directions of the flight passes during mission 5. To the right is a table explaining the geometry for each flight pass. Individual targets are marked with a number (1 to 25) and a list associates the target number with target type.

4. BASELINE PERFORMANCE

To facilitate development of new detection methods applied to the VHF image data set described in this paper, routines for reading and displaying the data have been implemented in Matlab. These routines will be distributed together with the image data set. A baseline change detection algorithm has also been implemented. This algorithm which is comprised of three parts; change analysis, CFAR normalization and detection analysis is the subject of the following subsections. Matlab was chosen as the development environment for this challenge problem based on its prominence as a code prototyping tool and for its ease in adding new functionality to the existing tools.

4.1 Input data

Input to the change detection algorithm are two geo-referenced magnitude SAR images covering the same ground area but acquired during different flight passes. These two images are referred to here as the surveillance and reference images. The goal is to combine the surveillance image with the reference image to suppress objects that are present in both images and enhance objects appearing in the surveillance image. Figure 8 shows an example of two images from the data set and a map covering the same area as the images. The image to the left is from mission 2 pass 1 where the 25 vehicles are deployed in forest 2 in deployment Sigismund. In the middle an image acquired during mission 4 pass 1 is shown. In this image target deployment Fredrik in forest 1 was used. Despite of the vehicles being concealed under foliage they appear as bright objects and can be discriminated from the background in both images. However, other structures such as power lines and fences also stand out from the background making it difficult to detect the targets in a single image with few false alarms.

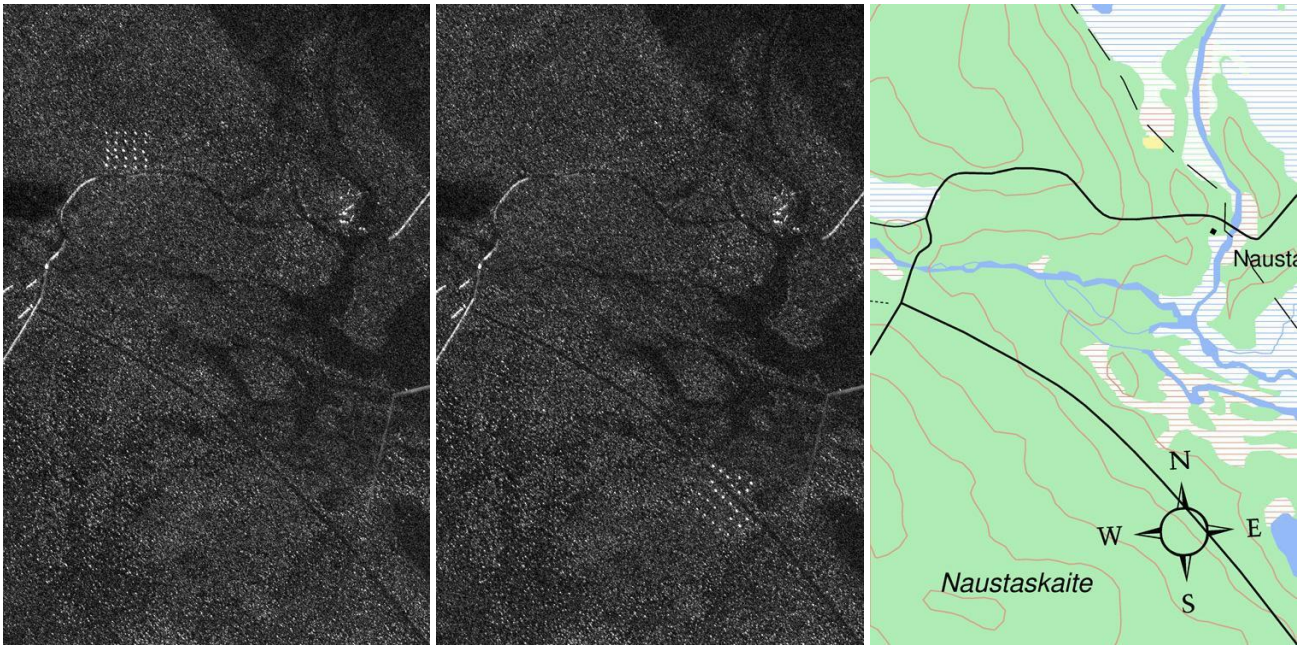

Figure 8. VHF SAR images of size 3 km x 2 km. Left: Image (v02_2_1_1.a.Fbp.RFcorr.Geo.Magn) with target deployment Sigismund in forest 2. Middle: Image (v02_4_1_1.a.Fbp.RFcorr.Geo.Magn) with target deployment Fredrik in forest 1. Right: Map covering the same area as the images. (© Map: Lantmäteriverket Gävle 2006. Ref. no. I 2006/719).

4.2 Change analysis

The change analysis method described here is based on the algorithm described in [11], which uses theory for space-time adaptive processing that exploits differences between target, clutter and interference signals in their space-time characteristics. Usually this technique is applied in GMTI (Ground Moving Target Indication) processing to combine data from several instantaneous receiving channels to suppress stationary clutter and detect moving targets. Here, the methodology is used to enhance changes between the two single channel SAR images acquired at different times. The problem is formulated as follows.

Let the target, clutter and noise signal be defined as:

$$\boldsymbol{s} = \begin{bmatrix} s_1 \\ s_2 \end{bmatrix} \qquad \boldsymbol{c} = \begin{bmatrix} c_1 \\ c_2 \end{bmatrix} \qquad \boldsymbol{n} = \begin{bmatrix} n_1 \\ n_2 \end{bmatrix}$$

Where the indices 1 and 2 refer to the two images. To determine if a change is present in the two channels (SAR images) a hypothesis test is used. The hypotheses are:

$$\begin{aligned} H_0 &: \quad \boldsymbol{z} = \boldsymbol{q} \quad (no\ change) \\ H_1 &: \quad \boldsymbol{z} = \boldsymbol{s} + \boldsymbol{q} \quad (change) \end{aligned}$$

The data from the two channels is denoted by $\boldsymbol{z}$ and the combined return from clutter and noise by $\boldsymbol{q} = \boldsymbol{c} + \boldsymbol{n}$. When no change has occurred the signal only contains contribution from clutter and noise. However, when a change is present the signal will also have a contribution from the target in one of the two channels. To test the two hypotheses a test statistic is computed. The algorithm uses the likelihood ratio test which maximizes probability of detection for a fixed false alarm rate. The test is defined by:

$$\Lambda(\boldsymbol{z}) = \mathbf{P}(\boldsymbol{z} \mid \boldsymbol{H_1}) / \mathbf{P}(\boldsymbol{z} \mid \boldsymbol{H_0})$$

P denotes the conditional probability under each hypothesis. To compute the test a statistical model is needed for the signal vector $\boldsymbol{z}$ that contains the two correlated magnitude SAR images. Despite of the data having only positive values Gaussian statistics is assumed. To reduce influence from noise the magnitude SAR image data is averaged with a low-pass filter before the test statistic is calculated. The averaging also has the benefit to improve the validity of the data being Gaussian distributed. The test statistic is then computed according to:

$$\Lambda(\boldsymbol{z}) = \boldsymbol{s}^T \boldsymbol{C}^{-1} \boldsymbol{z} \,/\, |\, \boldsymbol{s}^T \boldsymbol{C}^{-1} \boldsymbol{s}|$$

Where *T* denotes the transpose. The 2x2 covariance matrix denoted by $\boldsymbol{C}$, is estimated locally in the images using data from smaller image blocks. When the test statistics exceeds a certain threshold the $\boldsymbol{H_1}$ hypothesis is chosen. This threshold is related to the false alarm rate and will be determined later using a constant false alarm rate (CFAR) filter. The target signal is not known and must be assumed. Therefore, the assumption that a target is present in one image and not in the other is made:

$$\boldsymbol{s} = \begin{bmatrix} 0 \\ 1 \end{bmatrix} \quad \text{or} \quad \boldsymbol{s} = \begin{bmatrix} 1 \\ 0 \end{bmatrix}$$

When $\boldsymbol{s_1}$ is set to one and $\boldsymbol{s_2}$ is zero, image $\boldsymbol{z_1}$ is referred to as the surveillance image where new targets appear and image $\boldsymbol{z_2}$ as the reference image used for clutter suppression and vice versa.

Output from the change analysis step is a change image formed using the above test statistic.

4.3 CFAR normalization

After the change analysis, the next step in the change detection process is CFAR normalization. A normalized image is produced by applying a filter to the change image. The normalization is carried out to find an appropriate threshold that can be applied globally to give a constant probability of false alarms. A CFAR filter is used to estimate the local background statistics in the change image. The filter is defined as a convolution kernel with an outer frame containing non-zero values and an inner box with zeros, see Figure 9. The normalized image is produced by centering the filter at each pixel in the change image and estimate the mean and standard deviation for the pixels lying within the outer frame of the CFAR filter. This is done assuming Gaussian distributed data. The output CFAR image is computed by subtracting the mean value from the test pixel and divide by the standard deviation.

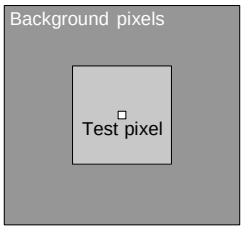

Figure 9. CFAR filter.

4.4 Detection analysis

The last step is to detect and find the coordinates of potential targets. A threshold is applied to the normalized CFAR image. This produces a binary image with detected objects. Following the threshold, two consecutive morphological operations are used in the binary image to reduce false detections. Based on the known resolution of the system (~3 m), erosion removes objects that are too small and dilation merges clusters of detections lying too close to each other. Finally, the coordinates of the detected objects are found by shrinking the remaining objects to the size of one pixel. Figure 10 shows the result when combining the two SAR images in Figure 8 using v02_2_1_1.a.Fbp.RFcorr.Geo.Magn as surveillance image and v02_4_1_1.a.Fbp.RFcorr.Geo.Magn as reference. To the left is the change image formed in the change analysis step and to the right is a detection image showing detected changes as white circles. In this example all 25 vehicles are detected but also one additional false detection is made.

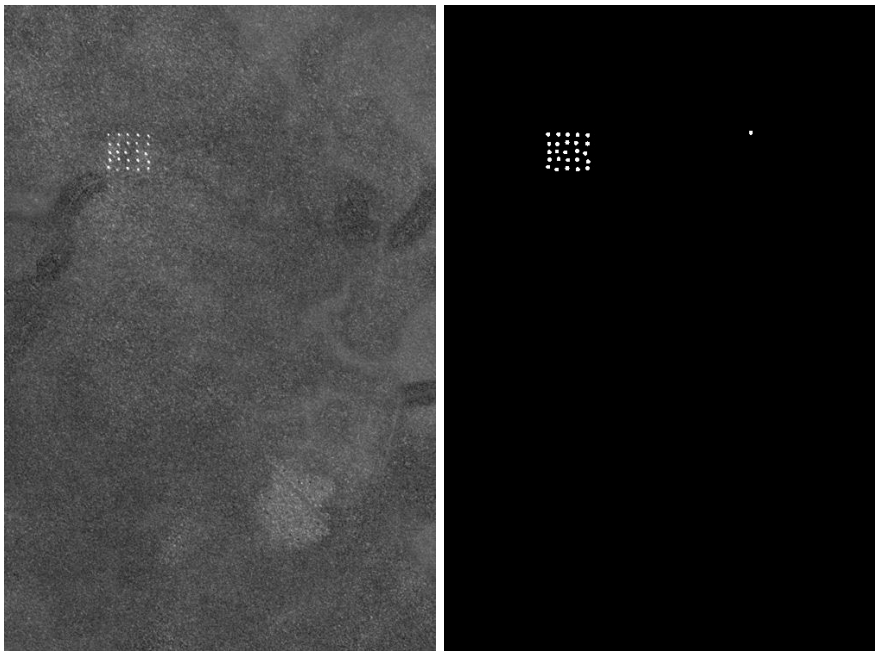

Figure 10. Change image (left) and detection image (right) showing the results when combining the surveillance image v02_2_1_1.a.Fbp.RFcorr.Geo.Magn and the reference image v02_4_1_1.a.Fbp.RFcorr.Geo.Magn shown in Figure 8.

4.5 Performance

To test the performance of the baseline algorithm 24 image pairs were run through the change detection process. For each image pair the detected changes were compared to the ground truth positions corresponding to the target deployment for the surveillance image. If detections existed within a radius of 10 m from the ground truth position, the target was declared to be found. Other detected changes that could not be related to any target were counted as false alarms. The metrics used to evaluate the performance are probability of detection and false alarm rate. Probability of detection is defined as number of detected targets divided by number of known targets. False alarm rate is here calculated as number of false alarms per square kilometer. These measures were calculated for one specific threshold in

the detection step. The results are summarized in Table 3, which includes a list of what image pairs were used and the performance for each image pair. Combining the results by using the accumulated values gave a total probability of detection of 97% and a false alarm rate of 0.67 false alarms per square kilometer. Table 4 specifies the parameters that were used in each processing step.

Table 3. Baseline change detection performance for 24 image pairs.

Surveillance image		Reference image		Number of known targets	Number of detected targets	Pd	Area	Number of false alarms	FAR
Mission	Pass	Mission	Pass				[km^2]		[km^-2]
2	1	3	1	25	25	1,00	6	2	0,33
3	1	4	1	25	22	0,88	6	1	0,17
4	1	5	1	25	25	1,00	6	2	0,33
5	1	2	1	25	23	0,92	6	4	0,67
2	2	4	2	25	25	1,00	6	2	0,33
3	2	5	2	25	25	1,00	6	4	0,67
4	2	2	2	25	25	1,00	6	3	0,50
5	2	3	2	25	25	1,00	6	4	0,67
2	3	5	3	25	25	1,00	6	3	0,50
3	3	2	3	25	23	0,92	6	4	0,67
4	3	3	3	25	25	1,00	6	0	0,00
5	3	4	3	25	24	0,96	6	2	0,33
2	4	3	4	25	24	0,96	6	3	0,50
3	4	4	4	25	25	1,00	6	2	0,33
4	4	5	4	25	25	1,00	6	4	0,67
5	4	2	4	25	25	1,00	6	4	0,67
2	5	4	5	25	25	1,00	6	3	0,50
3	5	5	5	25	17	0,68	6	10	1,67
4	5	2	5	25	25	1,00	6	2	0,33
5	5	3	5	25	23	0,92	6	29	4,83
2	6	5	6	25	25	1,00	6	1	0,17
3	6	2	6	25	25	1,00	6	3	0,50
4	6	3	6	25	25	1,00	6	1	0,17
5	6	4	6	25	23	0,92	6	3	0,50
Total				600	579	0,97	144	96	0,67

Table 4. Processing parameters used to produce test performance.

Processing step	Parameter	Value
Change Analysis	Block size	100 x 100 pixels
	Step size	10 pixels
	Averaging kernel size	5 x 5 pixels
CFAR Normalization	Kernel outer size	31 x 31 pixels
	Kernel inner size	19 x 19 pixels
Detection Analysis	Threshold	6
	Erode	1 time
	Dilate	2 times

5. CONCLUSIONS

We have presented a challenge problem for detecting targets under foliage using VHF-band SAR data. In the paper we defined the problem, described the provided CARABAS-II SAR image data set and presented the performance of a baseline change detection algorithm applied to this data set.

A copy of the VHF-band image data set can be requested from the AFRL Sensor Data Management System (SDMS) website at https://www.sdms.afrl.af.mil/.

REFERENCES

1. L.M.H. Ulander, W. Pierson, M. Lundberg, and A. Gustavsson, *Performance of VHF-band SAR Change Detection for Wide-Area Surveillance of Concealed Ground Targets*, Proc. SPIE vol. 5427, Algorithms for Synthetic Aperture Radar Imagery XI, held in Orlando, FL, 12-15 April 2004, pp. 259-270, 2004.

2. L.M.H. Ulander, P.-O. Frölind, A. Gustavsson, H. Hellsten, and B. Larsson, *Detection of Concealed Ground Targets in CARABAS SAR Images using Change Detection*, Proc. SPIE vol. 3721, Algorithms for Synthetic Aperture Radar Imagery VI, held in Orlando, FL, 5-9 April 1999, pp. 243-252, 1999.

3. H. Hellsten, L.M.H. Ulander, A. Gustavsson, and B. Larsson, *Development of VHF CARABAS II SAR*, Proc. SPIE vol. 2747, Radar Sensor Technology, held in Orlando, FL, 8-9 April 1996, pp. 48-60, 1996.

4. L.M.H. Ulander, *Performance of Stepped-Frequency Waveform for Ultra-Wideband SAR*, Proc. EUSAR'98, held in Friedrichshafen, Germany, 25-27 May 1998, pp. 323-326, 1998.

5. L.M.H. Ulander, B. Flood, P. Follo, P.-O. Frölind, A. Gustavsson, T. Jonsson, B. Larsson, M. Lundberg, W. Pierson, and G. Stenström, *Flight Campaign Vidsel 2002, CARABAS-II Change Detection Analysis*, FOI-R--1001--SE, Scientific Report, Swedish Defence Research Agency, 2003.

6. L.M.H. Ulander, B. Flood, P. Follo, P.-O. Frölind, A. Gustavsson, T. Jonsson, B. Larsson, M. Lundberg, and G. Stenström, *CARABAS-II Campaign Vidsel 2002. Flight Report*, FOI-R--1002--SE, Base Data Report, Swedish Defence Research Agency, 2003.

7. M. Lundberg, B. Flood, P. Follo, P.-O. Frölind, A. Gustavsson, T. Jonsson, B. Larsson, G. Stenström, and L.M.H. Ulander, *CARABAS-II Campaign Vidsel 2002. Ground Report*, FOI-R--0963--SE, Technical Report, Swedish Defence Research Agency, 2003.

8. F. Walter, *CARABAS-II Campaign Vidsel 2002. Forest Report*, FOI-R--0962--SE, Technical Report, Swedish Defence Research Agency, 2003.

9. F. Walter, J.E.S. Fransson, and P.-O. Frölind, *Fully Automatic Geo-coding of CARABAS-II VHF SAR Images*, Proc. IGARSS'99, held in Hamburg, Germany, 28 June - 2 July 1999, vol. 1, pp. 569-573, 1999.

10. P.-O. Frölind, L.M.H. Ulander, and A. Gustavsson, *Repeat-Pass VHF Interferometry Over Forest Covered Terrain*, Proc. EUSAR 2000, held in Munich, Germany, 23-25 May 2000, pp. 119-122, 2000.

11. L.M.H. Ulander, M. Lundberg, W. Pierson, and A. Gustavsson, *Change Detection for Low-Frequency SAR Ground Surveillance*, IEE Proc.-Radar Sonar Navig., Vol. 152, No. 6, pp. 413-420, December 2005.